Open Access

Hendrik Fullriede[a], Philipp Abendroth[a], Nina Ehlert, Katharina Doll, Jörn Schäske, Andreas Winkel, Sascha Nico Stumpp, Meike Stiesch and Peter Behrens*

pH-responsive release of chlorhexidine from modified nanoporous silica nanoparticles for dental applications

DOI 10.1515/bnm-2016-0003
Received February 2, 2016; accepted March 31, 2016

Abstract: A pH-sensitive stimulus-response system for controlled drug release was prepared by modifying nanoporous silica nanoparticles (NPSNPs) with poly(4-vinylpyridine) using a bismaleimide as linker. At physiological pH values, the polymer serves as gate keeper blocking the pore openings to prevent the release of cargo molecules. At acidic pH values as they can occur during a bacterial infection, the polymer strains become protonated and straighten up due to electrostatic repulsion. The pores are opened and the cargo is released. The drug chlorhexidine was loaded into the pores because of its excellent antibacterial properties and low tendency to form resistances. The release was performed in PBS and diluted hydrochloric acid, respectively. The results showed a considerably higher release in acidic media compared to neutral solvents. Reversibility of this pH-dependent release was established. In vitro tests proved good cytocompatibility of the prepared nanoparticles. Antibacterial activity tests with *Streptococcus mutans* and *Staphylococcus aureus* revealed promising perspectives of the release system for biofilm prevention. The developed polymer-modified silica nanoparticles can serve as an efficient controlled drug release system for long-term delivery in biomedical applications, such as in treatment of biofilm-associated infections, and could, for example, be used as medical implant coating or as components in dental composite materials.

Keywords: chlorhexidine; controlled drug delivery; dental application; pH-responsive release; silica nanoparticles; stimulus-responsive.

Introduction

Biofilm-associated diseases belong to the most important global health problems. A common attribute of bacteria organized in biofilms is their persistent nature and their increased resilience and resistance to external influences like antiseptics, antibiotics and host defenses [1]. In all medical disciplines bacterial biofilms can cause implant-associated infections, leading to loss of tissue and organ functions or even to the implant loss. In dentistry, biofilms cause caries and periodontitis, which are among the most common bacterial infections in humans [2]. For efficient prevention or treatment of biofilm infections several systems releasing antibacterial and remineralizing agents have been reported, e.g. fluoride (F^-) [3–6], calcium (Ca^{2+}) and phosphate (PO_4^{3-}) [7–10] or silver (Ag^+) ions [11, 12]. Chlorhexidine (CHX) is a widely applied drug because of its high antimicrobial activity against gram-positive and gram-negative bacteria, fungi and viruses [13]. In addition, the tendency to induce resistances is very low [14]. It is used as a preservative and in disinfectant products as well as in oral rinses [15]. Furthermore, CHX inhibits the formation of bacterial biofilms by binding to the enamel and pellicle. Thus, the accumulation of bacterial cells to these surfaces, which is the initial step in the formation of biofilms, is prevented [16]. CHX shows a high substantivity, which denotes the prolonged association with certain substrates, like the surfaces of teeth or mucosa within the

[a]**Hendrik Fullriede and Philipp Abendroth:** These authors contributed equally to this study.
***Corresponding author: Peter Behrens,** Gottfried Wilhelm Leibniz Universität Hannover, Institut für Anorganische Chemie, Callinstraße 9, 30167 Hannover, Germany, Phone: +49 511 762 3697, Fax: +49 511 762 3660, E-mail: peter.behrens@acb.uni-hannover.de
Hendrik Fullriede, Philipp Abendroth and Nina Ehlert: Institut für Anorganische Chemie, Gottfried Wilhelm Leibniz Universität Hannover, Hannover, Germany
Katharina Doll, Jörn Schäske, Andreas Winkel, Sascha Nico Stumpp and Meike Stiesch: Klinik für Zahnärztliche Prothetik und Biomedizinische Werkstoffkunde, Medizinische Hochschule Hannover, Hannover, Germany

oral cavity [17]. Therefore, CHX exhibits a reservoir effect. After a single rinse, CHX is able to reduce the salivary quantity of bacteria for several hours [16]. This made CHX to the gold standard for the prevention and treatment of microbial infections in dentistry [16].

Nanoporous silica materials have been investigated intensely, either as nanoparticles [18–21] or as implant surface coatings [22–25] since their first application as drug delivery platform in 2001 [26]. Nanoporous silica features various properties, which make this material interesting for a controlled release system. It offers high specific surface areas, large pore volumes and tunable pore sizes with narrow pore size distributions to allow high cargo loading. Nanoporous silica nanoparticles (NPSNPs), in particular, are of great interest to drug delivery, because their size [27–29], shape [30–35] and surface modification [36–38] can be adjusted. NPSNPs can easily be synthesized via the sol-gel route with surfactants as structure-directing agents [39]. These cytotoxic molecules are completely removable by calcination at high temperatures. Although, due to their high versatility and diversity, the toxicity assessment of NPSNPs still needs further investigation [40–43], NPSNPs are generally considered as safe in vitro and in vivo. The US Food and Drug Administration (FDA) recently has approved modified silica nanoparticles for clinical applications [44].

However, an uncontrolled leaching of antimicrobial substances from release systems has several disadvantages. While a burst release can be helpful for acute infections [23] and may be more effective than a prolonged delivery [45], there is a need for stimulus-responsive release systems, which are dormant for extended times, but will deliver cargo upon a certain trigger. Thus, the drug remains within the pores and is only extracted when necessary. Various stimuli were investigated, such as pH value [46–49], irradiation [50, 51], temperature [52, 53], redox potential [54], enzymatic activity [8] as well as specific antibodies [55] or glucose [56]. Systems using the irreversible cleavage of a chemical bond to remove pore-blocking gate keepers [57–59] only lead to a singular release that continues even after the stimulus has disappeared. A stimulus-responsive system working reversible would be more favorable for the desired long-term applications.

The approach, presented in this study, is to use the decrease of the pH value, as it can occur during an inflammation [60], as a practical internal trigger, thus providing an autarkic release system. By the post-synthetic modification of NPSNPs with poly(4-vinylpyridine) (PVP), a pH-sensitive release system can be generated [61]. PVP is commercially available with different chain lengths, so that cost- and time-consuming laboratory processes are

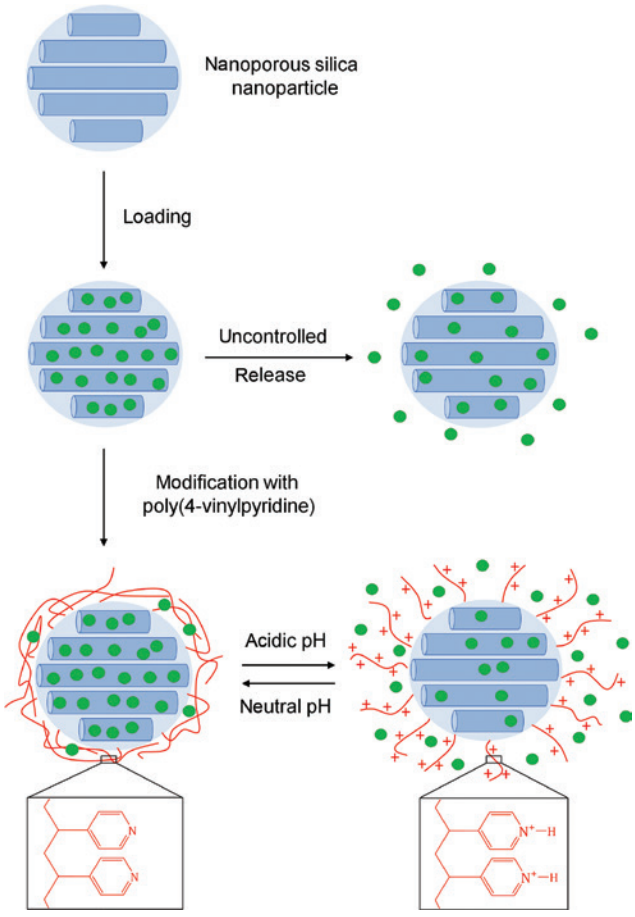

Figure 1: Illustration of uncontrolled and pH-responsive drug delivery systems based on nanoporous silica nanoparticles (NPSNPs). For controlled release NPSNPs were post-synthetically modified with poly(4-vinylpyridine).

not required. At neutral pH values, the polymer strains rest folded in a compact state around the NPSNPs (Figure 1). The pore openings are blocked and the drug molecules loaded into the pores remain there. At acidic pH values, the pyridine units of the polymer become protonated. The polymer strains straighten up because of repulsive interactions between the cationic pyridinium units and unseal the pores. The drug molecules can be released. After the successful treatment of a bacterial infection, the pH values return to a physiological state leading to the deprotonation of the polymer strains, which again block the pores, saving remaining agents.

A possible application of this system is the contact area between a dental restoration and the natural tooth, where bacteria like *Streptococcus mutans* would provoke a locally decreased pH by acid production during an infection.

Here, we present the development and the characterisation of a new stimulus-responsive drug release system on the base of NPSNPs. Furthermore, we tested

all components of the material with regard to their biocompatibility and carried out first investigations on the antibacterial properties against *Streptococcus mutans* (*S. mutans*), typically involved in dental caries, and *Staphylococcus aureus* (*S. aureus*), a major acidogenic pathogen associated with implant infections.

Results

Modified nanoporous silica nanoparticles

The nanoporous silica nanoparticles (NPSNPs) were synthesized according to an adapted literature procedure of Neumann and co-workers [29, 39]. They exhibited a spherical morphology and a narrow polydispersity with a mean diameter of 40 nm (Figure 2).

Dynamic light scattering (DLS) measurements confirmed these results and indicated a favorable low agglomeration tendency in ultrapure water (Supporting information). In the XRD pattern (Supporting information) a single broad reflection occurred at around 1.8° 2Θ, indicating a non-ordered pore structure for NPSNPs. Nitrogen sorption measurements showed a specific BET surface area of 1500 $m^2 g^{-1}$, a pore volume of 1.1 $cm^3 g^{-1}$ and a narrow pore width distribution with mean size of 3.6 nm.

For the construction of a controlled drug delivery system, the NPSNPs were modified with an amino-bismaleimide linker system and the pH-responsive polymer poly(4-vinylpyridine) (PVP). The progress of these reactions was easily monitored by infrared (IR) spectroscopy (Figure 3).

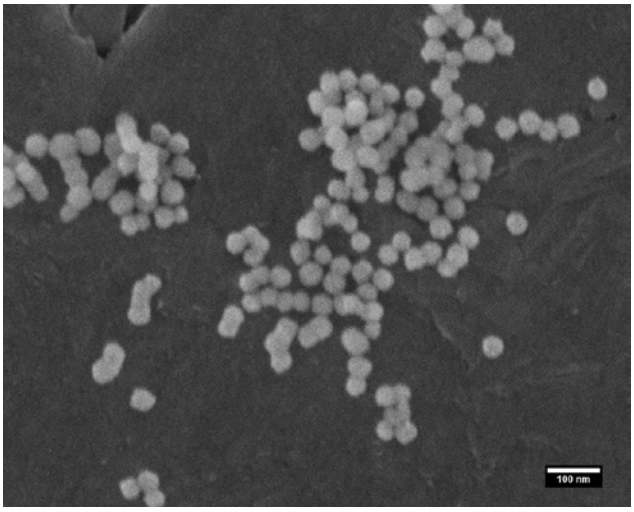

Figure 2: Scanning electron micrograph of nanoporous silica nanoparticles.

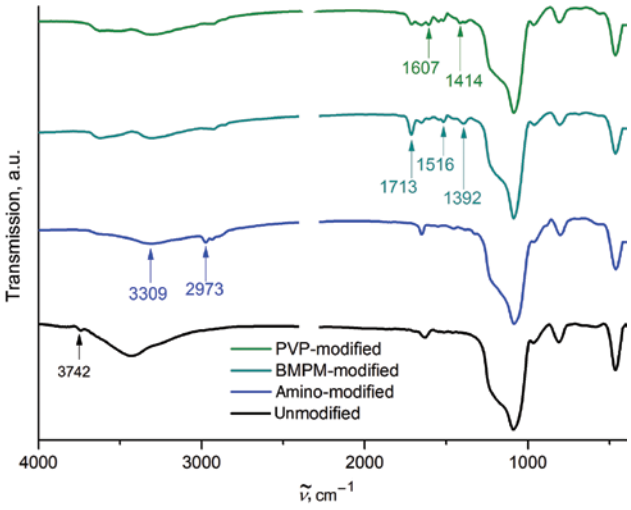

Figure 3: Infrared spectra of unmodified, amino-modified, bismaleimide-modified (BMPM-modified) and poly(4-vinylpyridine)-modified (PVP-modified) nanoporous silica nanoparticles.

As expected, all spectra showed characteristic IR absorption bands of silica in the region from 1000 to 1300 cm^{-1}. The broad band in the range of 3750 cm^{-1} to 2800 cm^{-1} corresponds to the O-H stretching vibration of water molecules hydrogen-bonded to surface silanol groups or between each other. Its intensity strongly decreased after the silanization reaction with (3-aminopropyl)trimethoxysilane (APTMS). In addition, the band at 3742 cm^{-1}, corresponding to free silanol groups [62], vanished after the reaction with APTMS. This reaction introduces primary aminopropyl groups, which gave rise to a broad band centered at 3309 cm^{-1}, corresponding to the N-H stretching vibration. Further bands between 2980 cm^{-1} and 2850 cm^{-1} are assigned to symmetric and asymmetric C-H stretching vibrations of the propyl residue [63].

PVP was attached to the amino-modified particles using 1,1′-(methylenedi-4,1-phenylene)bismaleimide (BMPM). The α,β-unsaturated carbonyl compound with two nucleophilic groups can react via a Michael addition with amino groups (Figure 4).

After the treatment with BMPM the IR spectrum exhibited additional bands at 1713 cm^{-1} (C=O stretching vibration), 1516 cm^{-1} (aromatic C=C stretching vibration) and 1392 cm^{-1} (C-N-C stretching vibration) [64]. The final modification with PVP (Figure 4B) resulted in further bands at 1607 and 1414 cm^{-1} corresponding to the pyridine groups [65]. After modification with PVP, the specific BET surface area dropped to 110 $m^2 g^{-1}$ and the pore volume to 0.1 $cm^3 g^{-1}$, respectively. These extensive reductions indicate a pore blocking caused by the PVP strains.

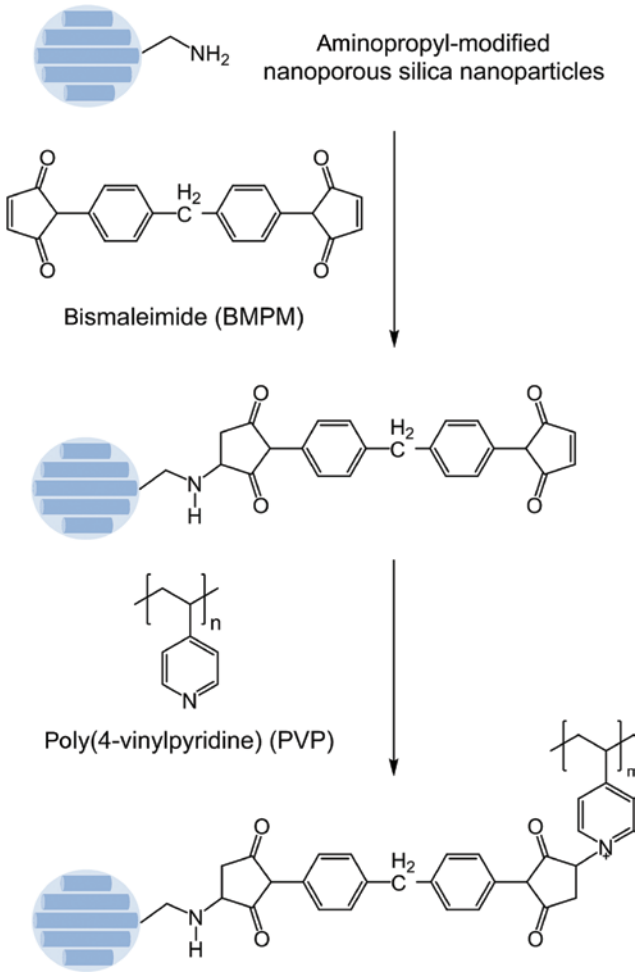

Figure 4: Michael addition reactions between surface-bound amino group and the bismaleimide BMPM and the now attached BMPM residue and the polymer poly(4-vinylpyridine) (PVP).

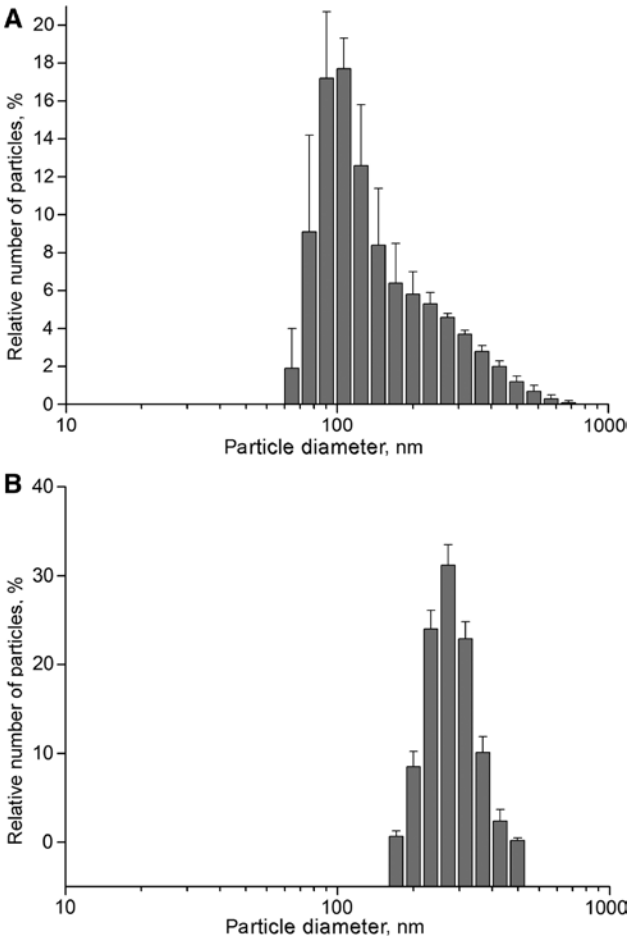

Figure 5: Dynamic light scattering measurements of poly(4-vinylpyridine)-modified nanoporous silica nanoparticles at (A) neutral (pH 7), and (B) acidic (pH 4) pH values. The polydispersity indices calculated by cumulant analysis are (A) PdI=0.584 and (B) PdI=0.312.

Measurements of zeta potential ξ of unmodified NPSNPs (Supporting information) revealed an isoelectric point at pH 4. At higher pH values the zeta potential of the particles became more negative due to the deprotonation of silanol groups. After modification with PVP the isoelectric point was shifted to a pH value of 7–8. At lower pH values, the modified particles are positively charged due to protonation of the pyridine groups and at higher pH values, possibly residual silanol groups become deprotonated.

The hydrodynamic diameter of the PVP-modified particles was determined in water and diluted hydrochloric acid to investigate the pH response of the polymer. At neutral conditions the mean size was approximately 100 nm with a slight increase of the polydispersity (Figure 5A) compared to the unmodified particles. The polydispersity index increases from PdI=0.511 to PdI=0.584 indicating in both cases a broad distribution. Under acidic conditions, at pH 4, the hydrodynamic diameter enlarged to 250 nm (Figure 5B), which can be ascribed to the straightening of the polymer strains due to protonation and the concomitant electrostatic repulsion. Interestingly, the polydispersity (PdI=0.312) became smaller in acidic solution, showing a nearly normal distribution of the particle diameter. Probably, the nanoparticles with the uncharged polymer corona tended to agglomeration, which is absent for the charged particles due to the electrostatic repulsion.

Loading and release of chlorhexidine

With regard to possible dental applications, chlorhexidine (CHX) was chosen for drug loading, because this antiseptic is currently the gold standard for the treatment

of infections in the oral cavity [16]. The loading of unmodified and PVP-modified NPSNPs was carried out with highly concentrated chlorhexidine gluconate stock solutions (118 mmol L^{-1}). The gluconate salt has a high solubility in water. Chlorhexidine dichloride solutions were tested as well, but gave significantly lower amounts of drug loading and release (results not shown). For loading PVP-modified NPSNPs, the pH value of the chlorhexidine gluconate solution had to be adjusted to pH 3 with *D*-gluconic acid in order to open the pores. After incubation of the particles in the stock solution for 3 days, the loaded amount was determined by thermogravimetry. Unmodified NPSNPs showed a content of 32 wt% CHX, PVP-modified NPSNPs incorporated 24 wt% CHX.

Besides the loading capacity, the release of incorporated agents is a key factor for the application as drug delivery system. The corresponding cumulative release curve of CHX from unmodified NPSNPs in PBS at pH 7.4 is shown in Figure 6. About 370 microgram of CHX per milligram of NPSNPs are released within 7 days in PBS. A burst release during the first 12 h was observed, followed by a nearly constant delivery of very small amounts.

After modification of NPSNPs with PVP, the burst released amounts of CHX in PBS at pH 7.4 were reduced to approximately 220 µg mg^{-1} (Figure 7). Afterwards, no further delivery of CHX was detectable. When adjusting to pH 4 with diluted hydrochloric acid, the released amount of CHX was considerably increased (Figure 7). This is the desired effect of the pH-responsive release. Furthermore, the release of PVP-modified nanoparticles loaded from a CHX solution was also studied at pH 5. The resulting

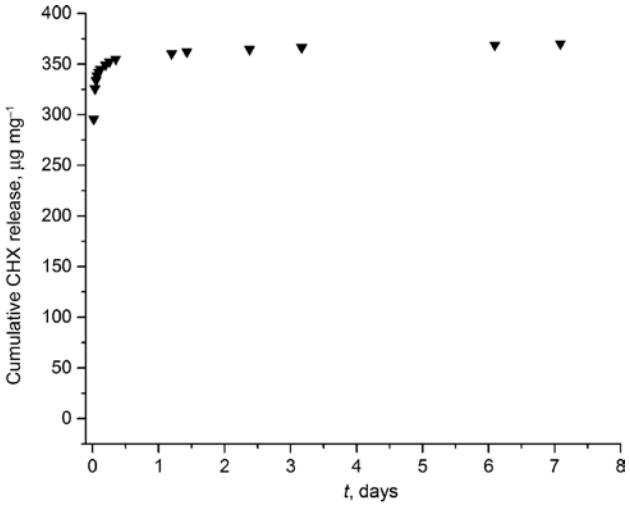

Figure 6: Cumulative release of chlorhexidine from unmodified nanoporous silica nanoparticles in phosphate buffered saline at pH 7.4 and 37 °C.

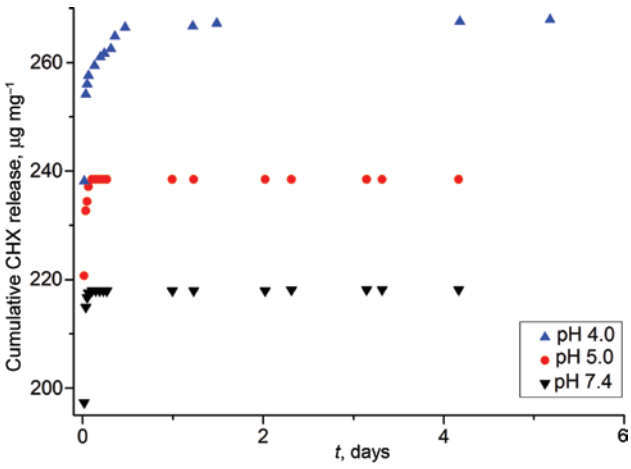

Figure 7: Cumulative release of chlorhexidine (CHX) from poly(4-vinylpyridine)-modified nanoporous silica nanoparticles in phosphate buffered saline (pH 7.4) and in aqueous hydrochloric acid solutions of different pH values.

curve was in between the curves at pH 7.4 and pH 4. Thus, the released amount of CHX correlates well with the pH value of the medium. We also note that with decreasing pH value, the system changes from a clear burst release behavior to a more gradual release kinetics. We ascribed the very strong burst release of the system at a pH value of 7.4 to the detachment of drug molecules from the polymer corona and the outer surface of the particles and therefore introduced additional washing steps in the further release studies.

The reversibility of the pH-responsive drug delivery system was investigated in detail using consecutive pH changes. For this purpose, PVP-modified NPSNPs loaded with CHX were dispersed in PBS at pH 7.4 for a certain time, separated from the solution by centrifugation and then re-dispersed in an aqueous hydrochloric acid solution at pH 4. This procedure was repeated several times and the corresponding release was monitored at every pH change (Figure 8). To eliminate the influence of the uncontrolled burst release observed at pH 7.4 (Figure 7) the PVP-modified NPSNPs were washed carefully before usage to remove all CHX which is potentially adsorbed on the polymer corona.

At physiological conditions the release rate was low, but it increased considerably at acidic pH values. The subsequent neutralization by redispersion in PBS leads to an almost complete stop of the release. Thus, the PVP-modified NPSNPs build up a reversible pH-sensitive release system. To release a higher amount of cargo, low pH values are necessary, as they can occur, e.g. during a bacterial infection.

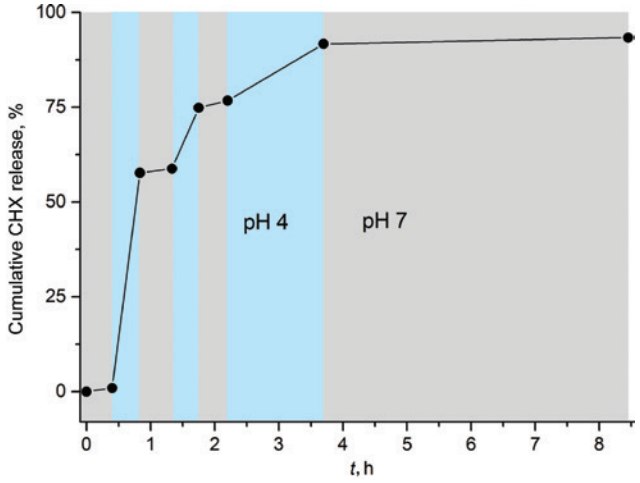

Figure 8: Verification of the reversibility of the release of chlorhexidine (CHX) from poly(4-vinylpyridine)-modified nanoporous silica nanoparticles by consecutive changes of the pH value from 7.4 (phosphate buffered saline, gray regions) to pH 4 (aqueous hydrochloric acid, blue regions).
Values were normalized to the final chlorhexidine concentration released in the experiment.

Cytocompatibility

The cytocompatibility of the drug delivery systems was tested by determining the metabolic activity of gingiva fibroblasts in cell cultures where the concentration of nanoparticles was increased stepwise. For this purpose, the unmodified and PVP-modified NPSNPs, respectively, were added to pre-cultured fibroblasts and incubated for 24 h. The metabolic activity was determined by using the well-established MTT assay, which is based on the cellular reduction of 3-(4,5-dimethylthiazol-2-yl)-2,5-diphenyltetrazolium bromide, and the LDH assay, which shows the cellular membrane damage by detecting lactate dehydrogenase from the inside of the cells.

Whereas the metabolic activity of fibroblasts in presence of NPSNPs (Figure 9) was similar to the control even at high concentrations, a loading with the antiseptic drug changed cellular response.

NPSNPs loaded with CHX revealed good cytocompatibility up to a concentration of 25 µg mL^{-1}. Above this value, the metabolic activity dramatically dropped to 10%. Due to these findings, the cytocompatibility was reviewed using lower particle concentrations (Figure 10).

The metabolic activity decreased with increasing nanoparticle concentration. The results of the LDH assay indicated a membrane damage of approximately 5% to 18%, which corresponded with the finding of the MTT assay.

After upgrading the uncontrolled drug delivery system to a controlled one by modification with the pH-responsive polymer PVP, the cytocompatibility was reviewed again (Figure 11).

Used directly, PVP-modified NPSNPs loaded with CHX posed a cytocompatibility which was comparable to that of the unmodified NPSNPs (Figure 11A) and bare CHX. To separate between the effects of the additional polymer coating and the antiseptic drug, the loaded PVP-modified NPSNPs were washed with PBS (pH 7.4) for 8 h and 1 week to remove potentially adsorbed chlorhexidine. The latter procedure was able to improve the cytocompatibility drastically up to a very high maximum concentration of 200 µg mL^{-1}. The results of the LDH assay corresponded very well to these findings, with no membrane damage detectable in the case of those nanoparticles which were washed for 1 week. Without long-term washing, the membranes of gingiva fibroblasts were damaged totally when the concentration of the loaded PVP-modified NPSNPs exceeded a concentration of 50 µg mL^{-1}.

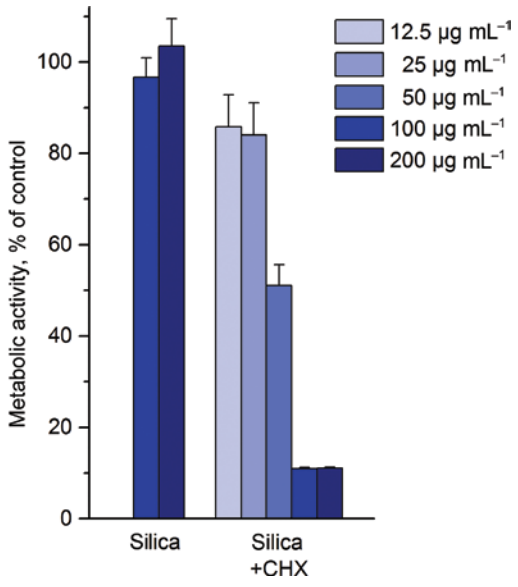

Figure 9: Cytocompatibility of bare (silica) and chlorhexidine-loaded unmodified nanoporous silica nanoparticles (silica+CHX) for gingiva fibroblasts showing the metabolic activity as determined by the MTT assay.

Antibacterial activity

For the investigation of the antibacterial activity of nanoparticles loaded with CHX, two human pathogens were chosen as model organisms. *S. mutans* is responsible for caries and secondary caries at dental fillings, whereas *S. aureus* is a major pathogen associated with implant-associated infections [66–68]. Both are aerobic, Gram-positive cocci.

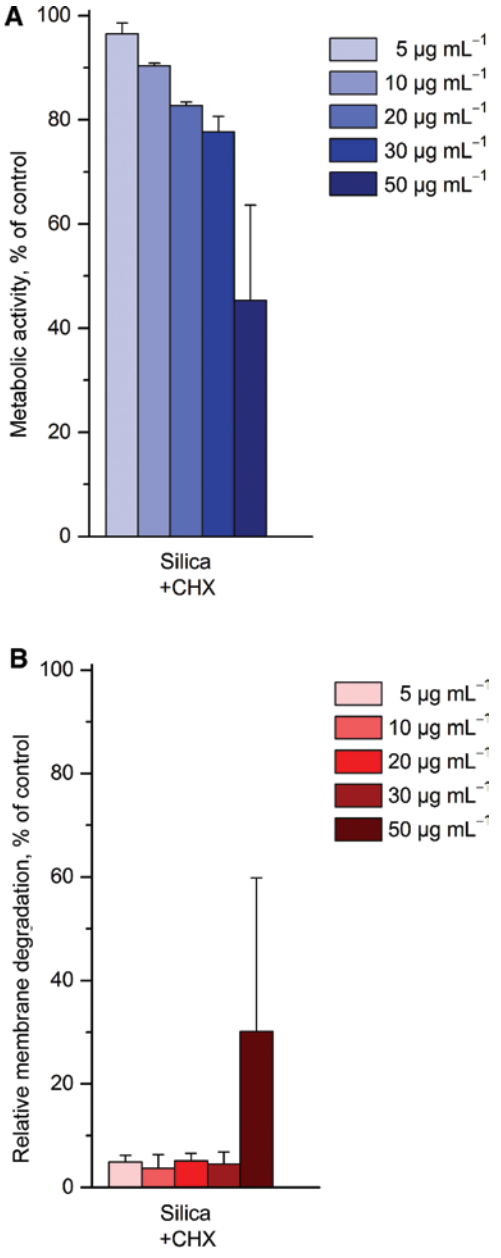

Figure 10: Review of cytocompatibility of nanoporous silica nanoparticles loaded with chlorhexidine (silica+CHX) for gingiva fibroblasts.
Evaluation of cellular response with regard to (A) metabolic activity, determined with the MTT assay; (B) membrane degradation, determined with the LDH assay.

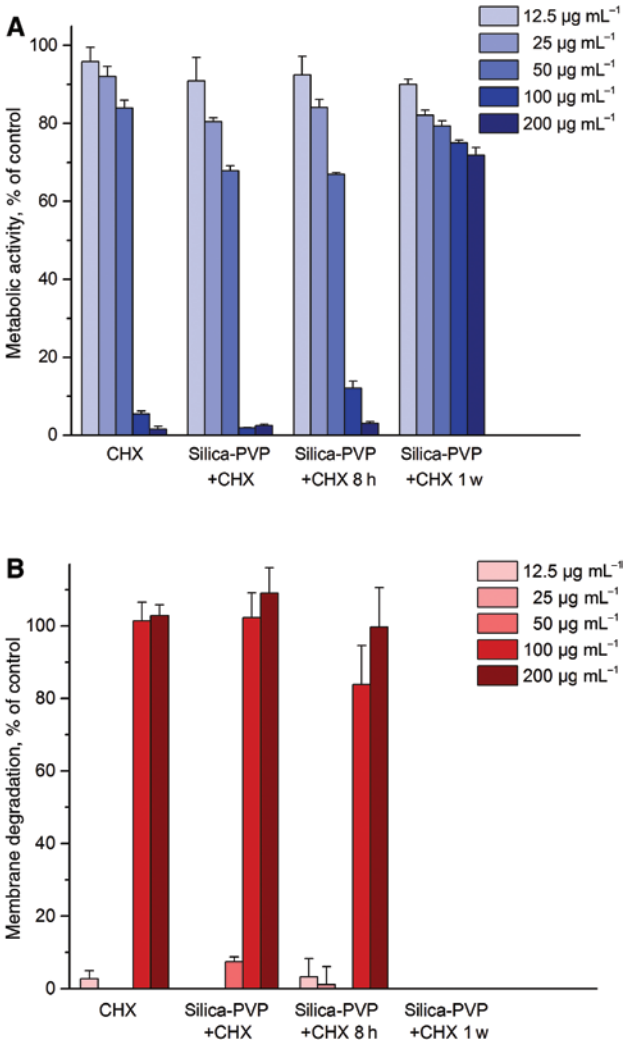

Figure 11: Cytocompatibility of chlorhexidine (CHX) and poly(4-vinylpyridine)-modified nanoporous silica nanoparticles loaded with CHX (silica-PVP+CHX) for gingiva fibroblasts.
Evaluation of cellular response with regard to (A) metabolic activity, determined with the MTT assay; (B) membrane degradation, determined with the LDH assay. In order to avoid action from the non-intentional release of CHX adsorbed on the outer surface of the polymer-modified nanoparticles, the loaded PVP-modified NPSNP were washed additionally for eight hour (8 h) or 1 week (1 w). No membrane degradation was detectable for nanoparticles which had been washed for 1 week.

To determine the antibacterial efficacy of CHX-loaded NPSNPs, investigations on bacteria suspensions and matured biofilms (Figure 12) were carried out. The antibacterial activity was determined with the well-established resazurin assay. With regard to the previous cytocompatibility testing (Figures 9 and 10), concentration in the range of 5 µg mL^{-1} to 50 µg mL^{-1} were chosen.

The antibacterial efficiencies of CHX released from unmodified NPSNPs were negligible for the treatment of matured biofilms of *S. mutans* and *S. aureus*. Only for a concentration of 50 µg mL^{-1}, a slight decrease of the relative metabolic activity of *S. aureus* was observed. This changed dramatically when the loaded nanoparticles were added to bacterial suspensions, i.e. growing biofilms. Exceeding the concentration of 5 µg mL^{-1} of the CHX-loaded nanoparticles leads to total inhibition of bacteria, their relative metabolic activity dropping to less than 5%.

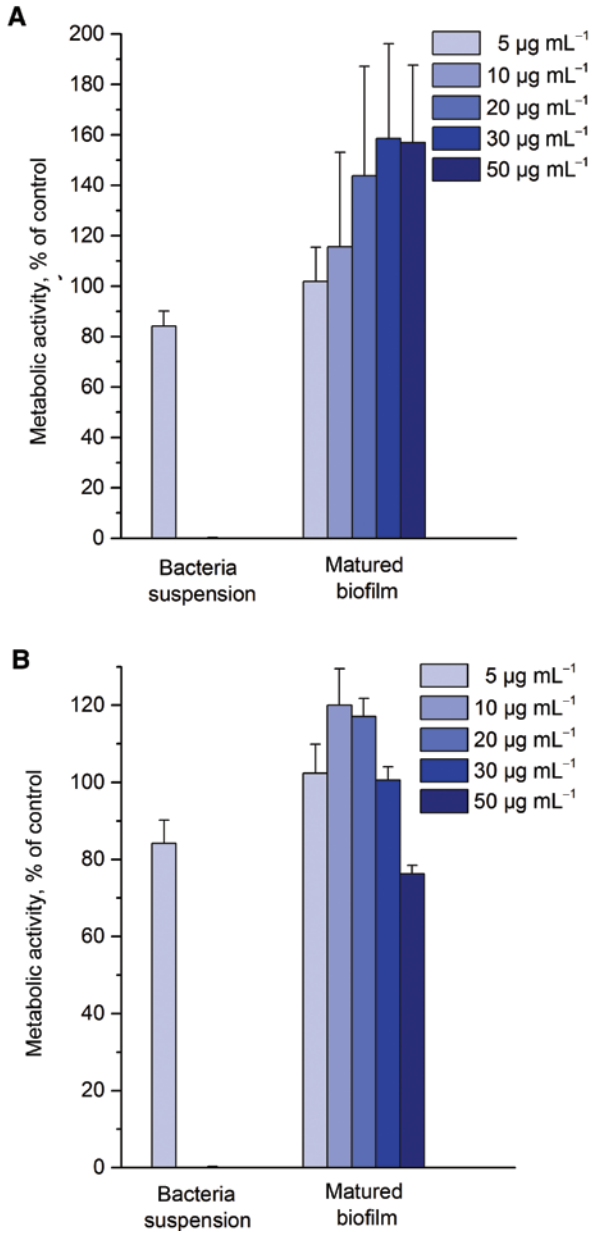

Figure 12: Antibacterial activity of unmodified nanoporous silica nanoparticles loaded with chlorhexidine against (A) *Streptococcus mutans* and (B) *Staphylococcus aureus* in bacteria suspensions and mature biofilms measured with the resazurin assay.

There were no significant differences observable between the two both bacterial species.

To assess the inducible antimicrobial activity of drug-loaded PVP-modified NPSNPs in response to a pH decrease, bacterial suspensions of either *S. aureus* or *S. mutans* were incubated with such NPSNPs. It can be seen from Figure 13 that disinfectant-bearing NPSNPs are active against both types of bacteria, inhibiting the bacterial growth completely except when used at the lowest concentration of 5 µg mL^{-1}. The action of the PVP-modified and CHX-loaded nanoparticles after several washing steps was reviewed in order to exclude antibacterial effects originating from uncontrolled CHX release from the polymer coating. It can clearly be seen that washing – either once or multiple times – does not significantly affect the antibacterial action against *S. mutans*. For *S. aureus* the same effect was observed, however only for NPSNPs concentrations higher than 50 µg mL^{-1}. During the bacterial cell culture experiments, we monitored the pH change of the medium. In experiments, where only PVP-modified NPSNPs without drug cargo were used, bacterial growth of *S. mutans* and *S. aureus* was observed resulting in a downshift of the pH value to 5.5 and 6. In those experiments, where the metabolic activity or viability of the bacteria was low due to drug action, the pH value did not change significantly and remained neutral to slightly alkaline.

It thus becomes obvious that with the experimental set-up used here, for successfully combating a bacterial infection a sufficient amount of CHX had to be present in the culture at a neutral pH value. This could be a hint that actually CHX adsorbed in the polymer corona or leaching out of the pores is the effective agent.

Discussion

The aim of this study was the development of a controlled drug delivery system with antibacterial properties for clinical application. For this purpose, the antimicrobial agent should be released at acidic pH levels characteristic for caries and tissue inflammation sites [60]. The mutans streptococci and lactobazilli are able to secret organic acids as products of glycoside fermentation [69]. This triggers local acidification processes, which favors the colonization of further acid-tolerant pathogenic bacteria [69]. As releasable disinfectant agent the chlorhexidine gluconate (CHX) was chosen, because of its well-known and comprehensively investigated antiseptic efficacy against bacteria in the oral cavitity [70].

To enable a wide range of applications, we used biocompatible nanoporous silica as a base material for the design of the release system. It can be employed as a surface coating on implants or in the form of nanoparticles [41] which can be applied directly or as part of a composite material like dental fillings [71]. Within our study, we were able to synthesize monodisperse, non-agglomerating NPSNPs with a high BET surface area and a large pore volume as shown by the results of SEM, DLS and sorption measurements. The further subsequent modifications of the particles with the amino-bismaleimide linker system

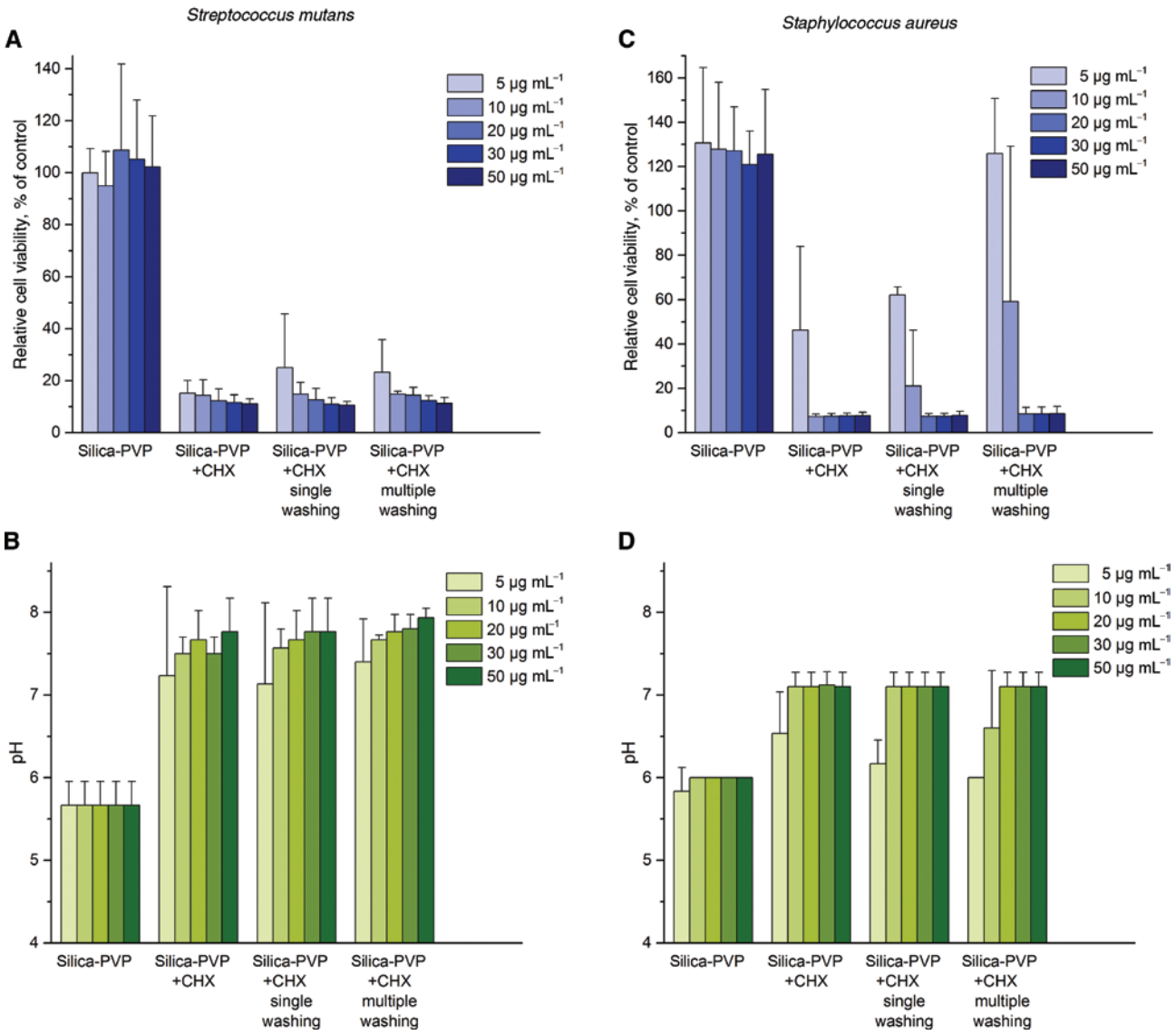

Figure 13: Antibacterial activity of as-manufactured and (single washing was carried out in PBS under ultrasonic treatment for 5 min followed by centrifugation, for multiple washing this procedure was carried out three times in total) poly(4-vinylpyridine)-modified NPSNPs loaded with CHX (silica-PVP+CHX) against (A) *Streptococcus mutans* and (C) *Staphylococcus aureus* and the corresponding pH values of the cell cultures of (B) *Streptococcus mutans* and (D) *Staphylococcus aureus*. Antibacterial activity was measured with resazurin assay.

APTMS-BMPM and the pH-responsive polymer poly(4-vinylpyridin) (PVP) were proven by the corresponding bands in the IR spectra and the increase of particle diameter of 100 nm appearing in DLS investigations. An additional extensive reduction of accessible BET surface area to 7.3% of the initial value and the smaller pore volume indicated the desired pore blocking caused by the PVP corona on the outer surface of the NPSNPs.

For unmodified NPSNPs, zeta potential measurements showed an isoelectric point of 4 and a negative charge of the particles arising at higher pH values due to the deprotonation of silanol groups. After modification with PVP, the isoelectric point was shifted to a pH value in the range of 7–8. Thus, at physiological pH values the polymer strains appear to remain nearly unprotonated. These results are close to those of other studies [72, 73], but differ somewhat due to the different constitution of the PVP-modified nanoparticles. We observe a higher isoelectric point as in those studies which may be caused by a more complete coverage of the NPSNPs with PVP. At lower pH values the zeta potential of the PVP-modified NPSNPs became more positive because of the increasing protonation of the pyridine groups. DLS measurements under neutral and acidic conditions demonstrated that

the particle hydrodynamic diameter increased to about 150% when the particles were placed in an acidic solution, due to the protonation and the concomitant electrostatic repulsion the polymer strains. This result indicates a close packing of the PVP molecules at neutral pH and an expansion of the polymer strains under acidic conditions. All these results showed the general suitability for a pH-responsive release.

By simple immersion procedures, we were able to incorporate a high amount of the CHX into NPSNPs. Thermogravimetric analysis revealed a high loading of 32 wt% CHX for unmodified and 24 wt% CHX for PVP-modified NPSNPs. With the exception of Zhang and co-workers, who were able to incorporate even 62.9 wt% of chlorhexidine diacetate into nanoporous SBA-15 particles [20], our values were much higher or very close to the findings of other studies [74, 75]. The slight decrease of the loading after modification with PVP is caused by the additional mass of the polymer corona. Thermogravimetric analysis indicated a polymer content of approximately 20 wt%.

All types of particles loaded with CHX show a very high initial burst release, releasing a high amount of cargo at the beginning even at physiological pH values. The only exception are PVP-modified NPSNPs which were washed for 1 week before testing. Due to the high incubation concentrations of CHX, an extensive amount of agent may be absorbed in the polymer coating of particles and become released within the first minutes of the experiment. The initially released amount of CHX from unmodified NPSNPs corresponds to a concentration of 1.6 mg mL^{-1} in the release medium; for PVP-modified NPSNPs, the corresponding concentration amounts to 1.3 mg mL^{-1}. These values are nearly one order of magnitude higher than the minimal inhibitory concentrations (MICs) for the tested bacterial species (1.6 μg mL^{-1} for *S. aureus* and 2.5 μg mL^{-1} for *S. mutans*) [76, 77]. After the burst release, all curves showed a nearly constant release with similar slopes. This leads to the assumption that the release depended on time rather than on the amount of incorporated CHX. In contrast to unmodified nanoparticles, the release of CHX from PVP-modified NPSNPs was controllable. Low pH values of pH 4 or pH 5 lead to a clear enhancement of CHX in the medium, whereas at pH 7.4, no significant additional release is observed after the initial burst release. The reversibility of the release system was tested by switching between pH values of 7 and 4 (Figure 8). A fast and well-defined answer of the system was observed. The amounts of CHX delivered in the intervals at pH 4 during later steps decreased with every step of pore opening (Figure 8), which is due to the fact that in the series of burst releases at pH 4, the concentration of CHX stored in the nanoparticles decreased. Therefore, with the combination of NPSNPs as host material and PVP as a pH-responsive gate keeper, a fast and reversible stimulated release system can be constructed.

We investigated possible cytotoxic effects caused by NPSNPs and chlorhexidine on gingiva fibroblasts to ensure the cytocompatibility in the concentration range of interest. As shown in Figure 9, only CHX-loaded unmodified NPSNPs exhibited cytotoxic effects. With regard to the well described good cytocompatibility of silica nanoparticles and the cytotoxicity of CHX on gingiva fibroblasts, the antiseptic drug is most likely responsible for the adverse effects on the cells [78]. Only a maximum concentration of 25 μg mL^{-1} for unmodified NPSNPs loaded with CHX could guarantee cytocompatibility. A detailed study revealed a clear relationship between the concentration and the metabolic activity of gingiva fibroblasts (Figure 11). The LDH assay indicated that CHX caused a minor damage of cell membranes, which corresponded to the result of the MTT assay. For PVP-modified NPSNPs loaded with CHX, the results of the cytocompatibility testings were very similar. The system is cytocompatible up to a concentration of 25 μg mL^{-1}. However, the cytocompatibility could be considerably improved by additional washing steps to remove drugs adsorbed on the outer surface or in the polymer corona of the nanoparticles. After washing for 1 week at neutral pH, the nanoparticles are cytocompatible up to very high concentrations of 200 μg mL^{-1}.

Unmodified NPSNPs loaded with CHX were effective against both bacterial strains tested. This could be explained by the high loading capacity and solubility of CHX in aqueous media. NPSNPs themselves had no antibacterial effects indicating a good setup for our investigations. In detailed investigations on the antibacterial effect with concentrations higher than 5 μg mL^{-1}, a strong antibacterial effect against suspensions of *S. mutans* and *S. aureus* was observed. In contrast, for mature biofilms no antibacterial effect could be detected. Biofilms are known to be highly tolerant against antimicrobials [79]. However, the reduced antibacterial effect of CHX may also be caused by a pH depended efficacy of the antiseptic drug. A proposed mode of action of CHX is the interaction of the drug molecule, which is positively charged under neutral pH conditions, and membrane of bacteria, which is negatively charged [6, 15]. Under acidic conditions, these membranes may be partly protonated, which reduces the interaction with CHX [76, 80]. In most cases, the optimum pH range for CHX applications is given as pH 5.5 to pH 7, but this varies with the type of organism and buffer [76, 77, 80]. It is known that the antibacterial activity of CHX against *S. aureus* and *Escherichia coli* increases

with rising pH value, whereas the effect on *Pseudomonas aeruginosa* (*P. aeruginosa*) is reversed [76]. In contrast, an in vitro study did not demonstrate any influence on the antibacterial efficiency of chlorhexidine digluconate in the range of pH 5.0–pH 9 against *S. aureus* and *P. aeruginosa* [6].

The cytocompatibility of PVP-modified NPSNPs is maintained up to a concentration of 25 μg mL^{-1} and could be further improved by washing for 1 week. PVP-modified NPSNPs loaded with CHX exhibited antibacterial effects when applied with concentrations higher than 5 μg mL^{-1}. However, for acidogenic *S. mutans*, no pH downshift was observed after incubation with CHX loaded nanoparticles. This indicates an antibacterial activity from the early beginning without bacterial growth and acidification of culture medium. The reason may be an uncontrolled release of adsorbed CHX. For *S. aureus*, no antibacterial effect of pH-responsive NPSNPs could be expected. It is a non-acidogenic bacterium so that the pH level does not fall below pH 6 during cultivation. This is insufficient for the induction of drug release. However, an antibacterial effect for concentrations higher than 5 μg mL^{-1} was observed which strengthens the hypothesis of unspecific CHX leaching.

Summarizing, the biological evaluation of the developed NPSNPs shows that the therapeutic window of our drug delivery systems, where fibroblasts stay vital whereas bacterial growth is inhibited, depends strongly on the number and the constitution of bacteria to combat. Unmodified NPSNPs loaded with CHX are applicable in the range 10 μg mL^{-1}–20 μg mL^{-1}. Currently, the pH-controlled release has to be optimized for the proposed biomedical applications. For example, a chemical crosslinking, which compresses the polymer corona, or extended washing could prevent the unwanted release at physiological pH.

Conclusion

To construct a pH-sensitive stimulus-response release system, PVP was attached to amino-modified NPSNPs by the use of an APTMS-BMPM-based linker system. CHX was successfully loaded into the particles by incubation from an acidified solution of its gluconate salt, leading to high amounts of adsorbed drug. The functionality of the system was proven by the successive exchange of release media with altering pH values of 4 and 7.4, showing a fast and reversible release behavior. This proves the general suitability of the system for a stimulus-responsive and repeated release with high reversibility. Furthermore, we were able to determine therapeutic windows for CHX loaded in unmodified and PVP-modified NPSNPs by detailed investigation of the cytocompatibility and the antibacterial effect. First antibacterial experiments with PVP-modified NPSNPs indicated some leaching effects under cell culture conditions, probably liberated from the outer surface or the polymer shell. This finding demands for further improvements towards a clinical application. This study, however, documents a proof-of-principle for the generation of pH-stimulus responsive nanoparticles loaded with antibacterial agents and could serve as a promising basis for the development of biofilm-inhibiting biomaterials.

Statement of authors

This study is a proof-of-principle for a self-sufficient controlled drug delivery system for the local treatment of biofilm-associated infections. We have established a reversible, pH-responsive release system for the antiseptic agent chlorhexidine. This system can be triggered by the acidic milieu present in infections of acid-producing bacteria, which play an important part during the formation of secondary caries and inflammations in the oral cavity. Using a novel, cost and time-saving approach, NPSNPs were stepwise modified with commercially available aminosilane, bismaleimide and the pH-responsive polymer poly(4-vinylpyridine). With the occurrence of an acidic pH value, the polymer chains become protonated, stretch and repel each other and open the gates to the drug reservoir. With detailed associated cytocompatibility and antibacterial activity testing in vitro, we were able to monitor the development and the efficacy of the system which however will still need further development, for example with regard to prohibiting unintentional release of drug adsorbed on the polymer shell of the particles.

Acknowledgments: This work was funded by the Deutsche Forschungsgemeinschaft as part of the Collaborative Research Center SFB 599 (project D12) and by the research initiative “Biofabrication for NIFE”. The authors thank Natalja Wendt and Jann Lippke (Gottfried Wilhelm Leibniz Universität Hannover) for carrying out the sorption measurements, Katharina Nolte and Sergej Springer (Gottfried Wilhelm Leibniz Universität Hannover) for thermogravimetric analysis and Dr. Britta Hering (Gottfried Wilhelm Leibniz Universität Hannover) for performing the SEM imaging. Gratitude also goes to Prof. Dr. Henning Menzel (Technische Universität Braunschweig) for scientific support in the field of polymers.

References

1. Mah TF, O'Toole GA. Mechanisms of biofilm resistance to antimicrobial agents. Trends Biotechnol. 2001;9:34–9.
2. Kolenbrander PE, Palmer RJ, Rickard AH, Jakubovics NS, Chalmers NI, Diaz PI. Bacterial interactions and successions during plaque development. Periodontol 2000. 2006;42:47–79.
3. Chan WD, Yang L, Wan W, Rizkalla AS. Fluoride release from dental cements and composites: A mechanistic study. Dent Mater. 2006;22:366–73.
4. Shen C. Controlled release of fluoride in connection with dental composite resins. Biomaterials. 1985;6:383–8.
5. Glasspoole EA, Erickson RL, Davidson CL. A fluoride-releasing composite for dental applications. Dent Mater. 2001;17:127–33.
6. Wiegand A, Buchalla W, Attin T. Review on fluoride-releasing restorative materials – fluoride release and uptake characteristics, antibacterial activity and influence on caries formation. Dent Mater. 2007;23:343–62.
7. Xu HH, Moreau JL, Sun L, Chow LC. Nanocomposite containing amorphous calcium phosphate nanoparticles for caries inhibition. Dent Mater. 2011;27:762–9.
8. Xu J-H, Gao F-P, Li L-L, Ma HL, Fan Y-S, Liu W, et al. Gelatin-mesoporous silica nanoparticles as matrix metalloproteinases-degradable drug delivery systems in vivo. Microporous Mesoporous Mater. 2013;182:165–72.
9. Xu H, Weir M, Sun L. Nanocomposites with Ca and PO4 release: Effects of reinforcement, dicalcium phosphate particle size and silanization. Dent Mater. 2007;23:1482–91.
10. Langhorst SE, O'Donnell J, Skrtic D. In vitro remineralization of enamel by polymeric amorphous calcium phosphate composite: quantitative microradiographic study. Dent Mater. 2009;25:884–91.
11. Yoshida K, Tanagawa M, Atsuta M. Characterization and inhibitory effect of antibacterial dental resin composites incorporating silver-supported materials. J Biomed Mater Res. 1999;47:516–22.
12. Chatzistavrou X, Fenno JC, Faulk D, Badylak S, Kasuga T, Boccaccini AR, et al. Fabrication and characterization of bioactive and antibacterial composites for dental applications. Acta Biomater. 2014;10:3723–32.
13. Horner C, Mawer D, Wilcox M. Reduced susceptibility to chlorhexidine in staphylococci: is it increasing and does it matter? J Antimicrob Chemother. 2012;67:2547–59.
14. Gilbert P, McBain AJ. Potential impact of increased use of biocides in consumer products on prevalence of antibiotic resistance. Clin Microbiol Rev. 2003;16:189–208.
15. McDonnell G, Russell D. Antiseptics and disinfectants: activity, action, and resistance. Clin Microbiol Rev. 1999;12:147–79.
16. Jones CG. Chlorhexidine: is it still the gold standard? Periodontol 2000. 1997;15:55–62.
17. Carrilho MR, Carvalho RM, Sousa EN, Nicolau J, Breschi L, Mazzoni A, et al. Substantivity of chlorhexidine to human dentin. Dent Mater. 2010;26:779–85.
18. Tao Z, Toms B, Goodisman J, Asefa T. Mesoporous silica microparticles enhance the cytotoxicity of anticancer platinum drugs. ACS Nano. 2010;4:789–94.
19. Kwon S, Singh RK, Perez RA, Abou Neel EA, Kim H-W, Chrzanowski W. Silica-based mesoporous nanoparticles for controlled drug delivery. J Tissue Eng. 2013;4:1–18.
20. Zhang JF, Wu R, Fan Y, Liao S, Wang Y, Wen ZT, et al. Antibacterial dental composites with chlorhexidine and mesoporous silica. J Dent Res. 2014;93:1283–9.
21. Tao Z. Mesoporous silica-based nanodevices for biological applications. RSC Adv. 2014;4:18961–80.
22. Ehlert N, Badar M, Christel A, Lohmeier SJ, Luessenhop T, Stieve M, et al. Mesoporous silica coatings for controlled release of the antibiotic ciprofloxacin from implants. J Mater Chem. 2011;21:752–60.
23. Lensing R, Bleich A, Smoczek A, Glage S, Ehlert N, Luessenhop T, et al. Efficacy of nanoporous silica coatings on middle ear prostheses as a delivery system for antibiotics: an animal study in rabbits. Acta Biomater. 2013;9:4815–25.
24. Ehlert N, Mueller PP, Stieve M, Lenarz T, Behrens P. Mesoporous silica films as a novel biomaterial: applications in the middle ear. Chem Soc Rev. 2013;42:3847–61.
25. Duda F, Bradel S, Bleich A, Abendroth P, Heemeier T, Ehlert N, et al. Biocompatibility of silver containing silica films on Bioverit® II middle ear prostheses in rabbits. J Biomater Appl. 2015;30:17–29.
26. Vallet-Regí M, Balas F, Arcos D. Mesoporous materials for drug delivery. Angew Chem Int Ed. 2007;46:7548–58.
27. Fowler CE, Khushalani D, Lebeau B, Mann S. Nanoscaled materials with sesostructured interiors. Adv Mater. 2001;13:649–52.
28. Cai Q, Luo Z-S, Pang W-Q, Fan Y-W, Chen X-H, Cui F-Z. Dilute solution routes to various controllable morphologies of MCM-41 silica with a basic medium. Chem Mater. 2001;13:258–63.
29. Qiao Z-A, Zhang L, Guo M, Liu Y, Huo Q. Synthesis of mesoporous silica nanoparticles via controlled hydrolysis and condensation of silicon alkoxide. Chem Mater. 2009;21:3823–9.
30. Rambaud F, Vallé K, Thibaud S, Julián-López B, Sanchez C. One-pot synthesis of functional helicoidal hybrid organic-inorganic nanofibers with periodically organized mesoporosity. Adv Funct Mater. 2009;19:2896–905.
31. Huh S, Wiench JW, Yoo J-C, Pruski M, Lin VS-Y. Organic functionalization and morphology control of mesoporous silicas via a co-condensation synthesis method. Chem Mater. 2003;15:4247–56.
32. Yang L-P, Zou P, Pan C-Y. Preparation of hierarchical worm-like silica nanotubes. J Mater Chem. 2009;19:1843–9.
33. Chen S-Y, Tang C-Y, Chuang W-T, Lee J-J, Tsai Y-L, Chan JCC, et al. A facile route to synthesizing functionalized mesoporous SBA-15 materials with platelet morphology and short mesochannels. Chem Mater. 2008;20:3906–16.
34. Nuraje N, Su K, Matsui H. Catalytic growth of silica nanoparticles in controlled shapes at planar liquid/liquid interfaces. New J Chem. 2007;31:1895–8.
35. Schmidt-Winkel P, Lukens WW, Yang P, Margolese DI, Lettow JS, Ying JY, et al. Microemulsion templating of siliceous mesostructured cellular foams with well-defined ultralarge mesopores. Chem Mater. 2000;12:686–96.
36. Kamarudin N, Jalil AA, Triwahyono S, Salleh N, Karim AH, Mukti RR, et al. Role of 3-aminopropyltriethoxysilane in the preparation of mesoporous silica nanoparticles for ibuprofen delivery: effect on physicochemical properties. Microporous Mesoporous Mater. 2013;180:235–41.
37. Schwartz DK. Mechanisms and kinetics of self-assembled monolayer formation. Annu Rev Phys Chem. 2001;52:107–37.
38. Howarter JA, Youngblood JP. Optimization of silica silanization by 3-aminopropyltriethoxysilane. Langmuir. 2006;22:11142–7.

39. Neumann A, Christel A, Kasper C, Behrens P. BMP2-loaded nanoporous silica nanoparticles promote osteogenic differentiation of human mesenchymal stem cells. RSC Adv. 2013;3:24222–30.
40. He Q, Zhang Z, Gao F, Li Y, Shi J. In vivo biodistribution and urinary excretion of mesoporous silica nanoparticles: effects of particle size and PEGylation. Small. 2011;7:271–80.
41. Tang F, Li L, Chen D. Mesoporous silica nanoparticles: synthesis, biocompatibility and drug delivery. Adv Mater. 2012;24:1504–34.
42. Asefa T, Tao Z. Biocompatibility of mesoporous silica nanoparticles. Chem Res Toxicol. 2012;25:2265–84.
43. Williams S, Neumann A, Bremer I, Su Y, Dräger G, Kasper C, et al. Nanoporous silica nanoparticles as biomaterials: evaluation of different strategies for the functionalization with polysialic acid by step-by-step cytocompatibility testing. J Mater Sci Mater Med. 2015;26:1–16.
44. Phillips E, Penate-Medina O, Zanzonico PB, Carvajal RD, Mohan P, Ye Y, et al. Clinical translation of an ultrasmall inorganic optical-PET imaging nanoparticle probe. Sci Transl Med. 2014;6:1–9.
45. Hesse D, Smoczek A, Glage S, Ehlert N, Luessenhop T, Müller PP, et al. Nanopouros silica coatings as a drug delivery system for ciprofloxacin: outcome of variable release rates in the infected middle ear of rabbits. Otol Neurotol. 2013;34:1138–45.
46. Lee C-H, Cheng S-H, Huang I-P, Souris JS, Yang C-S, Mou C-Y, et al. Intracellular pH-responsive mesoporous silica nanoparticles for the controlled release of anticancer chemotherapeutics. Angew Chem Int Ed. 2010;49:8214–9.
47. Zhang XF, Mansouri S, Clime L, Ly HQ, Yahia LH, Veres T. Fe3O4–silica core–shell nanoporous particles for high-capacity pH-triggered drug delivery. J Mater Chem. 2012;22:14450–7.
48. Schlossbauer A, Dohmen C, Schaffert D, Wagner E, Bein T. pH-responsive release of acetal-linked melittin from SBA-15 mesoporous silica. Angew Chem Int Ed. 2011;50:6828–30.
49. Zhao Y, Trewyn BG, Slowing II, Lin VS-Y. Mesoporous silica nanoparticle-based double drug delivery system for glucose-responsive controlled release of insulin and cyclic AMP. J Am Chem Soc. 2009;131:8398–400.
50. Guardado-Alvarez TM, Sudha Devi L, Russell MM, Schwartz BJ, Zink JI. Activation of snap-top capped mesoporous silica nanocontainers using two near-infrared photons. J Am Chem Soc. 2013;135:14000–3.
51. Lu J, Choi E, Tamanoi F, Zink JI. Light-activated nanoimpeller-controlled drug release in cancer cells. Small. 2008;4:421–6.
52. Kovačík P, Kremláčková Z, Štěpánek F. Investigation of radio-frequency induced release kinetics from magnetic hollow silica microspheres. Microporous Mesoporous Mater. 2012;159:119–25.
53. Mano JF. Stimuli-responsive polymeric systems for biomedical applications. Adv Eng Mater. 2008;10:515–27.
54. Chen L, Zheng Z, Wang J, Wang X. Mesoporous SBA-15 end-capped by PEG via l-cystine based linker for redox responsive controlled release. Microporous Mesoporous Mater. 2014;185:7–15.
55. Miyata T, Asami N, Uragami T. Structural design of stimuli-responsive bioconjugated hydrogels that respond to a target antigen. J Polym Sci B Polym Phys. 2009;47:2144–57.
56. Aznar E, Villalonga R, Giménez C, Sancenón F, Marcos MD, Martínez-Máñez R, et al. Glucose-triggered release using enzyme-gated mesoporous silica nanoparticles. Chem Commun. 2013;49:6391–3.
57. Chen X, Cheng X, Soeriyadi AH, Sagnella SM, Lu X, Scott JA, et al. Stimuli-responsive functionalized mesoporous silica nanoparticles for drug release in response to various biological stimuli. Biomater Sci. 2014;2:121–30.
58. Vivero-Escoto JL, Slowing II, Wu C-W, Lin VS-Y. Photoinduced intracellular controlled release drug delivery in human cells by gold-capped mesoporous silica nanosphere. J Am Chem Soc. 2009;131:3462–3.
59. Gan Q, Lu X, Yuan Y, Qian J, Zhou H, Lu X, et al. A magnetic, reversible pH-responsive nanogated ensemble based on Fe3O4 nanoparticles-capped mesoporous silica. Biomaterials. 2011;32:1932–42.
60. Steen KH, Steen AE, Reeh PW. A dominant role of acid pH in inflammatory excitation and sensitization of nociceptors in rat skin, in vitro. J Neurosci. 1995;15:3982–9.
61. Liu R, Liao P, Liu J, Feng P. Responsive polymer-coated mesoporous silica as a pH-sensitive nanocarrier for controlled release. Langmuir. 2011;27:3095–9.
62. Karabela M, Sideridou I. Effect of the structure of silane coupling agent on sorption characteristics of solvents by dental resin-nanocomposites. Dent Mater. 2008;24:1631–9.
63. Colilla M, Izquierdo-Barba I, Sánchez-Salcedo S, Fierro, JL, Hueso JL, Vallet-Regí M. Synthesis and characterization of zwitterionic SBA-15 nanostructured materials. Chem Mater. 2010;22:6459–66.
64. Xia B, Xiao S-J, Guo D-J, Wang J, Chao J, Liu H-B, et al. Biofunctionalisation of porous silicon (PS) surfaces by using homobifunctional cross-linkers. J Mater Chem. 2006;16:570–8.
65. Yang S, Zhao L, Yu C, Zhou X, Tang J, Yuan P, et al. On the origin of helical mesostructures. J Am Chem Soc. 2006;128:10460–6.
66. Pye AD, Lockhart D, Dawson MP, Murray CA, Smith AJ. A review of dental implants and infection. J Hosp Infect. 2009;72:104–10.
67. Islam B, Khan SN, Khan AU. Dental caries: from infection to prevention. Med Sci Monit. 2007;13:196–203.
68. Loesche W. Dental caries and periodontitis: contrasting two infections that have medical implications. Infect Dis Clin North Am. 2007;21:471–502.
69. Selwitz RH, Ismail AI, Pitts NB. Dental caries. Lancet. 2007;369:51–9.
70. Matthijs S, Adriaens PA. Chlorhexidine varnishes: a review. J Clin Periodontol. 2002;29:1–8.
71. Timpe N, Fullriede H, Borchers L, Stiesch M, Behrens P, Menzel H. Nanoporous silica nanoparticles with spherical and anisotropic shape as fillers in dental composite materials. BioNanoMaterials. 2014;15:89–99.
72. Percy MJ, Barthet C, Lobb JC, Khan MA, Lascelles SF, Vamvakaki M, et al. Synthesis and characterization of vinyl polymer-silica colloidal nanocomposites. Langmuir. 2000;16:6913–20.
73. Fujii S, Armes SP, Binks BP, Murakami R. Stimulus-responsive particulate emulsifiers based on lightly cross-linked poly(4-vinylpyridine)–silica nanocomposite microgels. Langmuir. 2006;22:6818–25.
74. Izquierdo-Barba I, Vallet-Regí M, Kupferschmidt N, Terasaki O, Schmidtchen A, Malmsten M. Incorporation of antimicrobial compounds in mesoporous silica film monolith. Biomaterials. 2009;30:5729–36.
75. Raso EM, Cortes ME, Teixeira KI, Franco MB, Mohallem NE, Sinisterra RD. A new controlled release system of chlorhexidine and chlorhexidine:βcd inclusion compounds based on porous silica. J Incl Phenom Macrocycl Chem. 2010;67:159–68.

76. Denton GW. Chlorhexidine. In: Block SS, editor. Disinfection, sterilization, and preservation. 5th ed. Philadelphia, PA, USA: Lippincott Williams & Wilkins, 2001: pp. 321–36.
77. Krämer I, Haber M, Duis A. Formulation requirements of the opthalic use of antiseptics. In: Kramer A, Behrens-Baumann W, editors. Antiseptic prophylaxis and therapy in ocular infections: principles, clinical practice and infection control; 68 tables. Basel, Switzerland: Karger Medical and Scientific Publishers, 2002: pp. 85–116.
78. Pucher JJ, Daniel JC. The effects of chlorhexidine digluconate on human fibroblasts in vitro. J Periodontol. 1992;63:526–32.
79. Davies D. Understanding biofilm resistance to antibacterial agents. Nat Rev Drug Discov. 2003;2:114–22.
80. Paulson DS. Handbook of topical antimicrobials: industrial applications in consumer products and pharmaceuticals. New York, USA: Marcel Dekker, 2003.

Supplemental Material: The online version of this article (DOI: 10.1515/bnm-2016-0003) offers supplementary material, available to authorized users.